

Disaster Impact Analysis Uses Land Cover Classification, Case study: Petobo Liquefaction

Rachmat Hidayat, Aniati Murni Arymurthy

Faculty of Computer Science

University of Indonesia

Depok, Indonesia

rachmat.hidayat92@ui.ac.id, aniati@cs.ui.ac.id

Dimas Sony Dewantara

Indonesian Institute of Sciences

Jakarta, Indonesia

dima008@lipi.go.id

Abstract—Analysis of changes in the conditions of an area can be done through satellite image analysis. This study utilizes the classification of satellite imagery to determine the impact of disasters and liquefaction disaster recovery efforts in the Petobo region, Palu, Central Sulawesi. The deep learning approach, namely Convolutional Neural Network (CNN) and CNN combined with ResNet as the Transfer Learning model, were selected as classification methods that would be compared in determining the approach with the best performance. The classification of satellite imagery is mapped into two main classes, namely natural land cover and artificial land cover. This research subsequently succeeded in mapping land cover changes that occurred as a result of liquefaction disasters and recovery efforts that have been carried out with promising performance

Keywords—disaster impact analysis, spatial data analysis, land cover classification, petobo liquefaction, convolutional neural network, resnet

I. INTRODUCTION

The earthquake that struck Palu on 28 October 2018 with a magnitude of 7.5 SR caused liquefaction in the Petobo region [1], [2]. Liquefaction is a phenomenon where the soil loses its density and starts flowing like a liquid. Liquefaction is a type of disaster caused by an earthquake that can cause fatalities and damage to infrastructure. Liquefaction has the potential to occur repeatedly [3]. Analysis of the conditions before, during, and after the liquefaction is essential to do. Like for analysis of the damage, and analysis of evaluation recovery process. Summary of changes in the status of an area can be done through image analysis; in this case, satellite imagery through mapping use and land cover [4], [5].

This research will apply an image-based classification approach through the use of deep learning, in this case, CNN. CNN currently has broad applications that include image classification, object detection, speech recognition, recommendation systems, natural language processing, and others [6][7][8]. Automatic feature extraction on CNN is carried out by utilizing a series of layers mainly composed of convolution layers, and pooling layers which function as filters of prominent or distinctive features in the data entered [9]. And then ResNet or residual network with transfer learning also used in this study. Transfer learning makes it possible to transfer pre-trained learning models to new models with different cases [10].

II. RELATED WORK

There have been many studies related to liquefaction disasters before. Liquefaction occurs when vibrations caused by earthquakes hit areas with low soil densities or soils that

contain a lot of water resulting in massive soil movements in the region [3]. Other research attempts to detect material overflow as a result of liquefaction. This study utilizes the use of satellite imagery with an object-based image analysis approach [11]. Other studies conducted the application of SAR analysis and optical images for the detection of seismic induction. This study uses image registration techniques to determine the changes that occur as a result of earthquakes and liquefaction [12]. The application of SAR analysis and optical images for detection of Liquefaction is also carried out in combination with the use of TDLI through the use of SWIR 1-2 in detecting liquefaction and affected areas [13]. These studies have the same limitations that can only identify the area affected by liquefaction.

Classification of land cover types before and after the liquefaction is needed to analyze the effects of the damage and evaluate the recovery efforts that have been made. This research will then analyze the effects of damage and analysis of post-disaster recovery efforts through the use of the classification of satellite images of liquefaction-affected areas with data retrieval time in three phases. The three phases are the phase before the disaster, the phase right after the disaster, and the current state of the affected area. The selection of the three phases is carried out to obtain an analysis related to the effects caused by the liquefaction and analysis related to the recovery efforts that have been made. Damage impact analysis is carried out through a comparison of conditions before and right after a disaster. In contrast, an analysis of recovery efforts is carried out by comparing conditions right after a disaster with the current situation of the affected area.

CNN and CNN deep learning approach with ResNet architecture as transfer learning were chosen as a method of classification of satellite images in this study. Both of these approaches have been widely used in image classification and have been shown to have excellent performance [14][15]. The dataset in this study utilizes a satellite image dataset with ten land cover classes [4], which are then grouped back into two major classes, natural land cover class, and artificial land cover class.

III. DATASET AND METHOD

The stages of the research process carried out in this study were three steps. First, pre-processing (cropping) dataset. Secondly, determine the model and architecture classification. Third, process data (training, and testing models). Fourth reunite the data/drawing test (re-arrange). And finally, the analysis of the impact of disasters and post-disaster recovery efforts that have been carried out using data comparisons between the time of the shooting. The stages in this research process can be seen in Fig. 1.

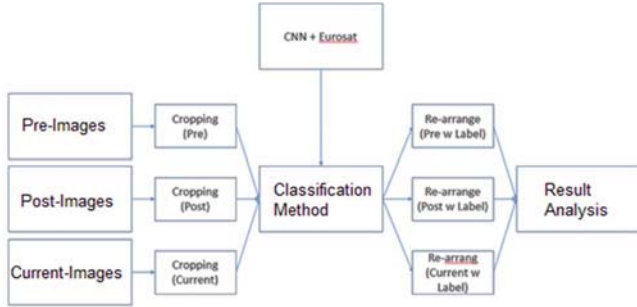


Fig. 1. Stages of Research

A. Dataset and Pre-processing

We use two datasets. First is the eurosat dataset[4], and the second is the standalone dataset created with Google Earth Imagery[16]. The eurosat dataset used to conduct training by dividing data into 80% for training, 20% for validation. This study grouped ten land cover classes in the eurosat dataset into two types, namely artificial land cover class, and natural land cover class. It is show in Fig. 2. The total land cover image used from the eurosat dataset is 10,000 images, with each class consisting of 5,000 images. For the testing process, we were using a standalone dataset obtained from the results of Google Earth satellite imagery with a time of taking the photo on 11/03/2018 for conditions before liquefaction (pre-images), taking the photo on 02/10/2018 for conditions shortly after liquefaction (post-images), and taking the photo on 06/11/2019 for the latest states that successfully obtained (current-images). Fig. 3 showing the data testing. These three images are cropping to match the size and resolution of the image in the training dataset. The examples of cropping images can be seen in Fig. 4.

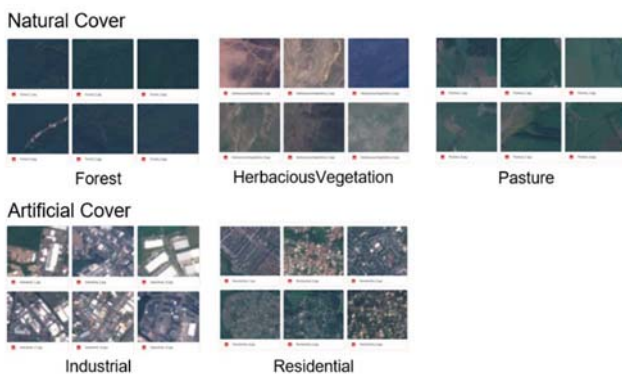


Fig. 2. Eurosat Dataset with Natural Cover and Artificial Cover



Fig. 3. Satellite Images of Areas Affected by the Petobo Liquefaction, Before a Disaster, Shortly After a Disaster, and Lastest States After a Disaster



Fig. 4. Examples of Cropping Images

B. CNN and ResNet Architecture

At this stage, the classification model will be determined. The classification model with a deep-learning approach, which is a 2-dimensional CNN, involves several process layers, including a 2-dimensional convolution layer and a pooling layer. Batch normalization also is carried out to reduce the possibility of overfitting in the model. ResNet as a transfer learning model is used to speed up the training process through the use of weights from the results of the training that have been done before, which are then stored for reuse so that further research does not need to conduct training processes from the beginning. ResNet is a residual learning framework to facilitate network training that is much deeper than existing neural networks. The advantage of ResNet is that it is easier to optimize and can improve accuracy based on depth [17]. This study further used ResNet50 as a transfer learning model used on the CNN approach with ResNet. The selected architectures can be seen in Fig. 5 and Fig. 6.

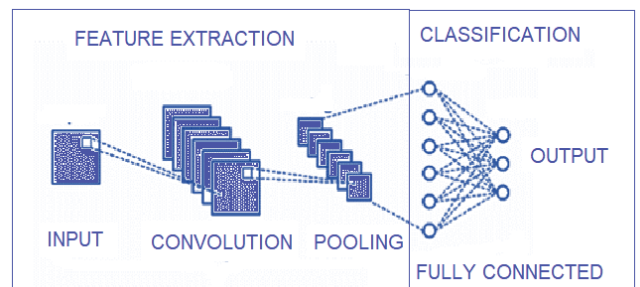


Fig. 5. CNN Architecture

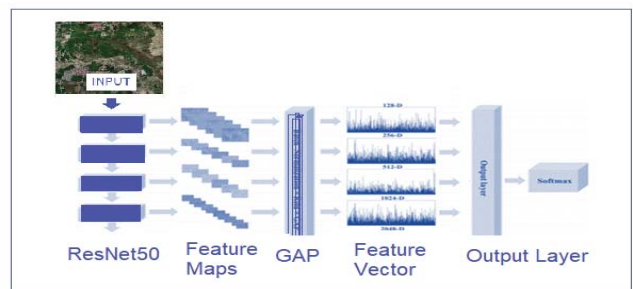


Fig. 6. ResNet Architecture

C. Land Cover Analysis

Through the approaches to the classification of satellite imagery in this study, distribution of land cover classes will be produced in 3 different periods. The distribution of land cover classes can then be compared based on the time taken to find out changes or transitions of land cover classes that occur. In this comparative process, two approaches can be used to determine the impact of damage and recovery efforts after liquefaction, namely by knowing the percentage change in artificial land cover to natural or otherwise natural to artificial. Furthermore, in this study, the impact of damage caused by liquefaction can be determined by reducing the grade of artificial land cover to natural conditions before the liquefaction compared to the terms immediately after the liquidation with the assumption that the area with artificial land cover class is reduced in this case the building is the impact of the liquefaction. While the evaluation related to post-liquefaction recovery efforts can be known through the addition of artificial land cover class from natural before on condition immediately after liquefaction compared to the current state after liquefaction based on the assumption of the additional area with land cover class, in this case, the building is the result of the recovery effort that has been done. Below is the formula used to calculate the percentage of land cover analysis:

- **Damage Impact = Percentage of artificial before liquefaction - Percentage of artificial shortly after liquefaction**
- **Recovery Effort = Percentage of recent artificial after liquefaction - Percentage of artificial shortly after liquefaction.**

IV. EXPERIMENT AND RESULT

In this section, we will conduct an impact analysis using the land cover classification. We did several experiments using two datasets, the eurosat dataset for the training stage and an independent dataset created with Google Earth as testing data. Eurosats dataset is used to conduct training by dividing data into 80% for training, 20% for validation, as for testing using a standalone dataset obtained from the results of Google Earth satellite imagery. There are three pictures with different shooting times to be classified, pictures of conditions before liquefaction took place on 11/03/2018, pictures of conditions shortly after liquefaction on 02/11/2018, and pictures of the latest states that were obtained on 06/11/2019. In testing, each image for testing is done rescale with a size of 1024 pixels x 512 pixels and then cropped into 64 pixels x 64 pixels to produce 128 images of cropping. All experiments were carried out using Google Colab in a GPU settings environment (Tesla K80, 12GB, 68 GB Disk Space).

A. Training and Testing Model

The training process is carried out using two approaches, namely CNN architecture and CNN, with ResNet50 with weights from Imagenet as transfer learning. Other settings used include optimizer using Adam, Loss Function using categorical_crossentropy, and ten epoch training. In this training process successfully obtained an accuracy value of 0.9752 for CNN and 0.9964 for CNN with ResNet50.

After the training process, we conducted a trial on sample data from cropping the image of the area affected by liquefaction obtained from Google Earth as a validation stage. We used 30 pieces of images from the test image and manually

labeled the 30 pictures. The results of this sample trial obtained the same classification accuracy value in both approaches of 0.9 for CNN and CNN with ResNet.

B. Experiment Result for Pre-images Classification (11/03/2018)

The results of the classification in the figure with the time taken before the liquefaction obtained a percentage of the natural land cover of 30.46875% and the artificial land cover of 69.53125% through the CNN approach without transfer learning. As for the CNN approach with ResNet50, the percentage of the natural land cover was 32.03125%, and the artificial land cover was 67.96875%. The results can be seen in Fig. 7 and Fig. 8 below.

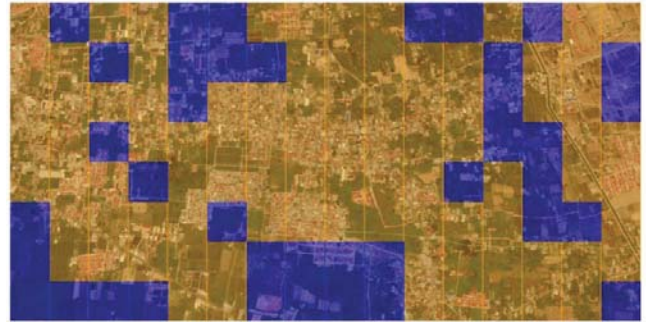


Fig. 7. CNN Result in First Phase

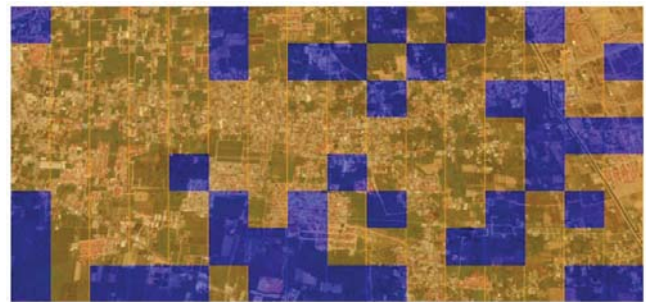


Fig. 8. ResNet Result in First Phase

C. Experiment Result for Post-images Classification (02/10/2018)

The results of the classification in the picture with the time taken just after the liquefaction obtained a percentage of the natural land cover of 54.6875% and the artificial land cover of 45.3125% through the CNN approach without transfer learning. As for the CNN approach with ResNet50, the percentage of the natural land cover was 49,21875%, and the artificial land cover was 50.78125%. The results can be seen in Fig. 9 and Fig. 10 below.

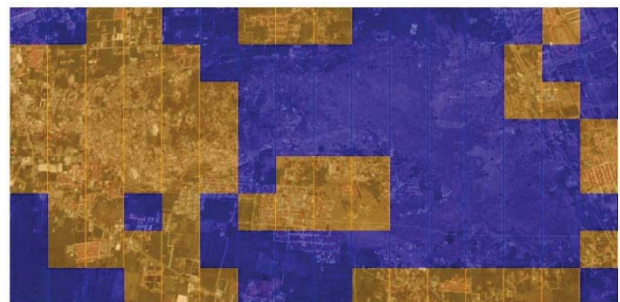


Fig. 9. CNN Result in Second Phase

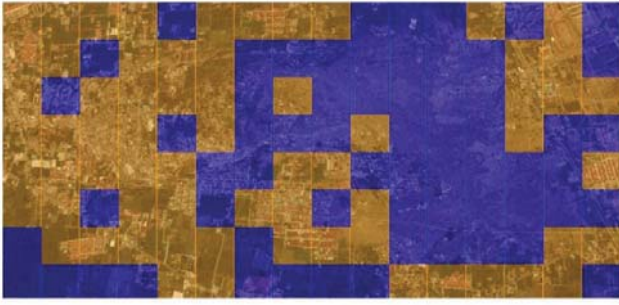


Fig. 10. ResNet Result in Second Phase

D. Experiment result for Current-images classification (06/11/2019)

The results of the classification in the picture with the time of taking the latest conditions after liquefaction obtained a percentage of the natural land cover of 78,125% and the artificial land cover of 21,875% through the CNN approach without transfer learning. As for the CNN approach with ResNet50, the percentage of the natural land cover was 68.75%, and the artificial land cover was 31.25%. The results can be seen in Fig. 11 and Fig. 12 below.

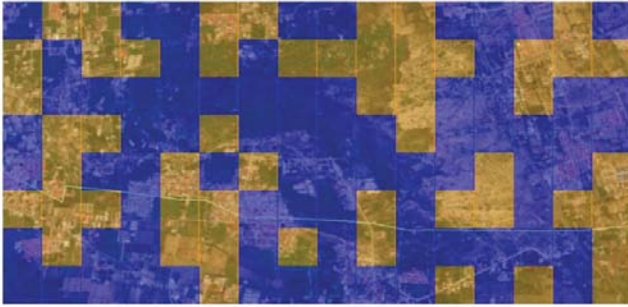


Fig. 11. CNN Result in Third Phase

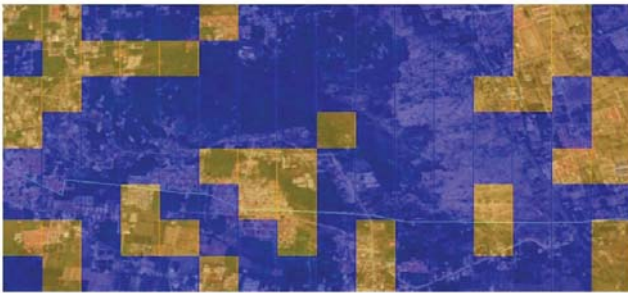


Fig. 12. ResNet Result in Third Phase

E. Analysis of the impact of damage and recovery efforts after liquefaction.

Damage impact analysis and post-liquefaction recovery efforts were carried out by finding the percentage change in the class area of artificial land cover between each time of the shooting. The analysis is carried out using the image-differencing technique, which is one of the changes in detection techniques [18]. The technique is used in the calculation formula as below:

$$DI = PABL - PASAL \quad (1)$$

$$RE = PRAL - PASAL \quad (2)$$

Denote:

- DI: Damage Impact
- RE: Recovery Effort
- PABL: % artificial classification before liquefaction (classification results in Fig. 7 and Fig. 8)
- PASAL: % artificial classification shortly after liquefaction (classification results in Fig. 9 and Fig.10)
- PRAL: % of the most recent artificial classifications after liquefaction (classification results in Fig. 11 and Fig. 12)

Based on experiments conducted, the PABL, PASAL and PRAL values are as follows:

1. With the CNN approach: PABL (69.53%), PASAL (45.31%) and PRAL (21.87%)
2. With the CNN + ResNet approach: PABL (67.96%), PASAL (50.78%) and PRAL (31.25%)

Then from the results of experiments and formula calculations, the results of the percentage of damage impacts and recovery efforts can be seen in Table 1.

TABLE I. ANALYSIS RESULT

Classification	Damage impacts (DI = PABL - PASAL)	Recovery effort (RE = PRAL - PASAL)
CNN	69.53% - 45.31% = 24.22%	21.87% - 45.31% = - 23.44%
CNN+ResNet50	67.96% - 50.78% = 17.18%	31.25% - 50.78% = - 19.53%

From the table above, observations can be made related to the percentage of land cover changes that occur. The impact of damage on both classification approaches both show a positive value indicating that there has been a decline in the area of artificial land cover class as a result of liquefaction. In contrast, the restoration efforts of the two classification approaches both showed negative values related to the addition of areas with the artificial land cover, which indicated that after the liquefaction, there was not much recovery effort. This may be intended as an effort to prevent damage if liquefaction occurs again in the area currently affected.

V. CONCLUSION

In this study, we use a deep-learning approach, namely CNN, and CNN, with transfer learning (ResNet50) as a method of image classification. Then, we are divide satellite imagery into two classes of land cover, natural and artificial. We use this classification of satellite images for analyzing the impact of damage and recovery efforts in the Petobo area, Palu, Central Sulawesi. The classification process is carried out in 3 time periods, namely before, a moment, and after a disaster. We are analysis of the impact of damage and recovery efforts with observations related to land cover class transitions that occurred between the time of taking satellite imagery. Through the result of this analysis, we concluded that liquefaction results in a decrease in the area of artificial land cover as a result of damage. While the recovery effort is not much done. We can see from the decline in areas with artificial land cover classes in the current condition.

This research can produce a description of the area affected liquefaction. Besides, this study can also determine the type of land cover class and the percentage of land cover changes that occur as a result of this disbursement disaster. In

the future, the results of this research can still be improved in several ways, especially the compatibility of the dataset in training with data during testing to improve classification accuracy. Also, it can be enhanced by selecting land cover classes by adding a class of "debris" in addition to the two previous classes, namely natural and artificial, which aim to facilitate the observation process.

REFERENCES

- [1] A. Yulianur, T. Saidi, B. Setiawan, S. Sugianto, M. Rusdi, and M. Affan, "Microtremor datasets at liquefaction site of Petobo, Central Sulawesi-Indonesia," *Data in Brief*, vol. 30, p. 105554, June 2020. doi: 10.1016/j.dib.2020.105554.
- [2] Y. Darma, B. Sulistyantara, and Yonvitner, "Analysis of Landscape Impact on Post-Earthquake, Tsunami, and Liquefaction Disasters in Palu City, Central Sulawesi". IOP Conference Series: Earth and Environmental Science, Bogor, Indonesia, vol. 501, p. 012003, June 2020. doi: 10.1088/1755-1315/501/1/012003.
- [3] Y. Zhang, "Risk analysis of soil liquefaction in earthquake disasters," *E3S Web of Conferences*, Shanghai, China, vol. 118, October 2019. doi: 10.1051/e3sconf/201911803037.
- [4] P. Helber, B. Bischke, A. Dengel, and D. Borth, "EuroSAT: A Novel Dataset and Deep Learning Benchmark for Land Use and Land Cover Classification," *IEEE Journal of Selected Topics in Applied Earth Observations and Remote Sensing*, vol. 12, pp. 2217-2226, July 2019. doi: 10.1109/JSTARS.2019.2918242.
- [5] S. Talukdar, P. Singha, S. Mahato, Shahfahad, S. Pal, Y. Liou, and A. Rahman, "Land-Use Land-Cover Classification by Machine Learning Classifiers for Satellite Observations—A Review," *Remote Sensing*, vol. 12, April 2020. doi: 10.3390/rs12071135.
- [6] R. Wason, "Deep Learning: Evolution and Expansion," *Cognitive Systems Research*, vol. 52, pp. 701-708, December 2018. doi: 10.1016/j.cogsys.2018.08.023.
- [7] Y. Kim, "Convolutional Neural Networks for Sentence Classification," *Proceedings of the 2014 Conference on Empirical Methods in Natural Language Processing*, Doha, Qatar, pp. 1746-1751, October 2014. doi: 10.3115/v1/D14-1181.
- [8] X. Cao, P. Wang, C. Meng, X. Bai, G. Gong, M. Liu, and J. Qi, "Region Based CNN for Foreign Object Debris Detection on Airfield Pavement," *Sensors*, vol. 18, p. 737, March 2018. doi: 10.3390/s18030737.
- [9] S. Albawi, T. A. Mohammed and S. Al-Zawi, "Understanding of a convolutional neural network," 2017 International Conference on Engineering and Technology (ICET), Antalya, Turkey, pp. 1-6, August 2017. doi: 10.1109/ICEngTechnol.2017.8308186.
- [10] M. Shaha and M. Pawar, "Transfer Learning for Image Classification," 2018 Second International Conference on Electronics, Communication and Aerospace Technology (ICECA), Coimbatore, India, pp. 656-660, March 2018. doi: 10.1109/ICECA.2018.8474802.
- [11] J. Morgenroth, M. Hughes, and M. Cubrinovski, "Object-based image analysis for mapping earthquake-induced liquefaction ejecta in Christchurch, New Zealand," *Natural Hazards*, vol. 82, pp. 763-775, February 2016. doi: 10.1007/s11069-016-2217-0.
- [12] M. Polcari, C. Tolomei, C. Bignami, and S. Stramondo, "SAR and Optical Data Comparison for Detecting Co-Seismic Slip and Induced Phenomena during the 2018 M w 7.5 Sulawesi Earthquake," *Sensors*, vol. 19, September 2019. doi: 10.3390/s19183976.
- [13] H. Baik, Y. Son, and K. Kim, "Detection of Liquefaction Phenomena from the 2017 Pohang (Korea) Earthquake Using Remote Sensing Data," *Remote Sensing*, vol. 11, p. 2184, September 2019. doi: 10.3390/rs11182184.
- [14] A. S. B. Reddy and D. S. Juliet, "Transfer Learning with ResNet-50 for Malaria Cell-Image Classification," 2019 International Conference on Communication and Signal Processing (ICCSP), Chennai, India, pp. 0945-0949, April 2019. doi: 10.1109/ICCSP.2019.8697909.
- [15] Z. Wu, C. Shen, and A. Van Den Hengel, "Wider or deeper: Revisiting the resnet model for visual recognition," *Pattern Recognition*, vol. 90, pp. 119-133, June 2019. doi: 10.1016/j.patcog.2019.01.006.
- [16] A. Nguyen, H. Luu, A. Phan, H. Bui, and T. Nguyen, "'Cau Giay: A Dataset for Very Dense Building Extraction from Google Earth Imagery," 2019 6th NAFOSTED Conference on Information and Computer Science (NICS), Hanoi, Vietnam, pp. 352- 356, December 2019. doi: 10.1109/NICS48868.2019.9023848.
- [17] K. He, X. Zhang, S. Ren and J. Sun, "Deep Residual Learning for Image Recognition," 2016 IEEE Conference on Computer Vision and Pattern Recognition (CVPR), Las Vegas, NV, pp. 770-778, June 2016. doi: 10.1109/CVPR.2016.90.
- [18] Karthik and B. R. Shivakumar, "Change detection using image differencing: A study over area surrounding Kumta, India, " 2017 Second International Conference on Electrical, Computer and Communication Technologies (ICECCT), Coimbatore, India, pp. 1-5, February 2017. doi: 10.1109/ICECCT.2017.8117851.